

## Physics studies to define the CMS muon detector upgrade for High-Luminosity LHC

L. BORGONOV<sup>(1)(2)(\*)</sup>

<sup>(1)</sup> *INFN, Sezione di Bologna - Bologna, Italy*

<sup>(2)</sup> *Dipartimento di Fisica, Università di Bologna - Bologna, Italy*

received 15 February 2017

**Summary.** — In view of the High-Luminosity phase of LHC, the CMS detector will undergo a major upgrade, the Phase-II Upgrade (2024), consequent to the Phase-I Upgrade (2019). To improve redundancy and extend the coverage to high pseudo-rapidity regions, the muon system will be equipped with new Micro Pattern Gaseous detectors. To understand the effects of the muon detector Phase-II Upgrade, Monte Carlo simulations reproducing different detector scenarios have been produced. Then the detector response to the Higgs reconstruction has been studied, analyzing Higgs boson decaying into four muons events. The results of the comparison between the different configurations are reported, together with considerations regarding the improvement given by the geometrical extension of the muon system to the Higgs reconstruction.

### 1. – Introduction

In 2012 the Higgs boson discovery was announced by the two main experiments at the CERN Large Hadron Collider (LHC): CMS and ATLAS [1, 2]. This result was the conclusion of several decades of extensive searches aimed at verifying the last missing piece of the Standard Model of particles and interactions (SM). In fact, in 1964 F. Englert, R. Brout and P. Higgs proposed a mechanism that explained the masses of the vector bosons  $W^\pm$  and  $Z^0$  through the Spontaneous Symmetry Breaking (SSB) of the electroweak theory. The so-called Higgs mechanism predicted the existence of a new scalar boson with unknown mass, whose couplings to fermions and bosons are the origins of their mass [3, 4].

Much of the future experimental program in particle physics will focus on measurements of the Higgs boson properties. In order to collect the high statistics needed for

---

(\*) E-mail: [lisa.borgonovi@bo.infn.it](mailto:lisa.borgonovi@bo.infn.it); [lisa.borgonovi2@unibo.it](mailto:lisa.borgonovi2@unibo.it)

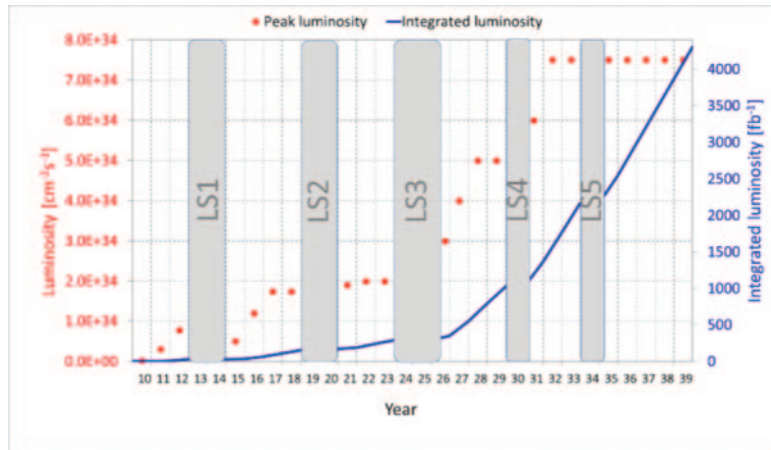


Fig. 1. – Scheme of the planning of shutdown and LHC performances for the next 20 years.

high-precision measurements, an upgrade program has been proposed for the LHC, increasing both energy and luminosity in the next twenty years, as reported in fig. 1. The first “long shutdown” period (LS1) has just finished and Run2 is ongoing, with LHC operating at a center-of-mass energy increased from 8 TeV (2012 - Run1) to 13 TeV. During the next shutdown (LS2), the CMS experiment will complete a substantial upgrade, referred to as Phase-I [5-7].

During the following LS3, scheduled in 2023, the LHC and the injection system will be substantially upgraded to reach luminosities as high as  $\mathcal{L} = 5 \times 10^{34} \text{ cm}^{-2}\text{s}^{-1}$ . This will allow, in a ten year operating period to collect an integrated luminosity of  $3000 \text{ fb}^{-1}$ . The high instantaneous luminosity will come at the price of an extremely high number of overlapping events (pile-up), up to 140 for a bunch-crossing interval of 25 ns. To cope with these new conditions, the CMS detector will also be upgraded: this second stage is called Phase-II [8,9].

In this context, it is mandatory to verify the performance of detectors damaged by radiation, and the impact of the upgrades on the main physics channels, as the “golden channel”,  $H \rightarrow ZZ^{(*)} \rightarrow 4\mu$ . This will help identifying what is needed to maintain good efficiency and event reconstruction, and the best technology to achieve this goal.

## 2. – The CMS detector

The Compact Muon Solenoid (CMS) [10,11] is, with ATLAS, a multi-purpose detector at the Large Hadron Collider (LHC) at CERN. It has a cylindrical structure, 21.6 m long with a diameter of 14.6 m and a total weight of approximately 14500 tons. In fig. 2 a schematic representation of the CMS detector, is reported. It can be divided in three main sections: i) barrel, the central region; ii) end-caps, the two regions orthogonal to the beam axis that hermetically close the barrel at both ends; iii) very forward regions, the sub-detectors very close to the beam axis *i.e.* at very high pseudo-rapidity values. From the inside-out, the detector presents the following sub-systems: the tracker, that allows the charged particles track reconstruction, electromagnetic and hadron calorimeters, used to identify the energy deposit of photons and electrons, and hadrons respectively, a solenoid magnet, that bends the particle tracks allowing charge and momentum identification, and

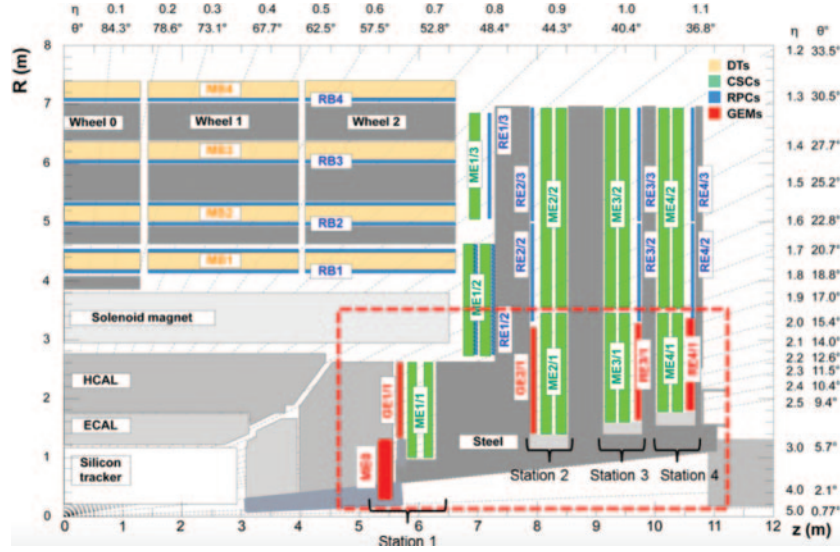


Fig. 2. – Longitudinal view of the CMS detector: planned detector for the muon system upgrades are marked in red.

the muon system with the iron “return yoke”, composed of different gas-detectors used to reconstruct muons. Collecting the information from the detectors, the trigger and data acquisition systems select and store event data, to make them accessible for the offline CMS reconstruction.

**2.1. The CMS Upgrades.** – The CMS physics program of the next decades is challenging, aiming at answering fundamental questions about the Standard Model, and exploring high-energy physics and very rare physics processes. As mentioned before, the LHC will undergo major upgrades in terms of instantaneous and integrated luminosity, which lead to a huge amount of overlapping pile-up events, expected to be up to 140: this will increase the probability of fake particle reconstruction and reduce the energy resolution capability. In order to cope with these unprecedented conditions, the CMS experiment will need to improve the detector ability to select and reconstruct the final states produced in the  $p$ - $p$  collisions: more granularity and redundancy is needed, to be able to distinguish the primary interactions from the pile-up ones. Furthermore, the aging of the detector-sensitive material due to radiation damage has to be addressed, since it will contribute to worsen the reconstruction performance. To be competitive and in the best conditions to produce consistent results, the CMS detector will be upgraded in two different steps, following the LHC upgrade program: the *Phase-I Upgrade*, which will be completed during the LS2 in 2019, and consisting in the upgrade of the internal pixel detector, the L1 trigger, and the electronics of the hadron calorimeter, and the *Phase-II Upgrade*, planned for the LS3 in 2024. This second upgrade, still under study, will include a major change in all sub-detectors, in order to cope with the challenging conditions of HL-LHC. In addition to the replacement of the tracker, the substitution of the forward calorimeters with a new High-Granularity calorimeter, and the improvement of the trigger and read-out electronics, the muon system will be upgraded adding new stations of muon detectors to improve the redundancy and the geometrical acceptance

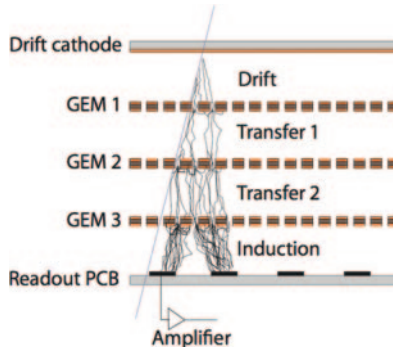


Fig. 3. – Structure of the Triple-GEM detector with three foils, a drift electrode on the top and a read-out electrode at the bottom defining drift and induction fields.

(extending the pseudo-rapidity coverage from  $|\eta| < 2.4$  to  $|\eta| < 2.8$ ). These new stations, called GE1/1, GE2/1 and ME0, will be realized using Micro Pattern Gaseous Detectors.

**2.2. Micro-Pattern Gaseous Detectors.** – Micro-Pattern Gaseous Detectors (MPGD) [12] are high-granularity gaseous detectors with a clear separation between ionization (drift) and amplification regions, and small distances between anode and cathode electrodes. The separation of the two regions improves the spatial resolution and the rate capability (with respect to classical gaseous detectors) since the avalanche is concentrated in the amplification region so that the charge can be evacuated more easily. On the other hand these detectors present a large discharge probability due to the small distance between the electrodes.

One of the most well known MPGD is the Gas Electron Multiplier (GEM) [13, 14], usually employed in the Triple GEM configuration: three ionization (drift) regions alternated to three GEM foils, as shown in fig. 3. A GEM foil is a thin polymer (Kapton) foil, cladded on both sides with copper ( $5\ \mu\text{m}$  thick), chemically perforated with bi-conical holes ( $70\ \mu\text{m}$  diameter,  $140\ \mu\text{m}$  pitch). Applying a different voltage to the sides of the foil, an intense electric field is created inside the holes, and this allows the amplification of the charge produced in the drift region. The read-out is then done at the end of the last stage of the Triple GEM. These detectors allow high rate capabilities ( $100\ \text{MHz}/\text{cm}^2$ ), high gain ( $> 10^4$ ), good efficiency ( $> 97\%$ ), high spatial ( $100\ \mu\text{m}$ ) and temporal ( $< 10\ \text{ns}$ ) resolution.

Starting from GEM detectors, other different types of MPGD have been developed, with modifications to the structure in order to improve the performance and/or the production stage. For example the  $\mu$ -RWell detector [15] presents a unique GEM foil glued directly to the read-out plane, through a resistive layer. This configuration helps in avoiding discharges and reduces the constructions costs and difficulties since the thin GEM foil has not to be stretched.

### 3. – The $H \rightarrow ZZ^{(*)} \rightarrow 4\mu$ channel

One of the main motivations for the construction of the LHC has been the Higgs boson discovery. In 2012, ATLAS and CMS discovered this new boson, studying the channels  $H \rightarrow \gamma\gamma$  and the  $H \rightarrow ZZ^{(*)} \rightarrow 4\ell$ . In particular, the Higgs boson decaying

into two  $Z$  bosons, each decaying into two charged leptons (electron or muons), has been named the “golden channel”. Thanks to the clean and clear final state composed of four isolated charged leptons which can be fully reconstructed in the detector, excellent efficiency, energy and momentum resolutions can be achieved. Measuring the angle between the  $ZZ$  decay planes and the decay angles in these planes, the  $CP$  properties of the Higgs boson can be assessed; moreover, the analysis of the four lepton invariant mass spectrum, and the production rate of the  $H \rightarrow ZZ^{(*)}$  decay can lead to information about the total width of the boson and possible deviations from the Standard Model. This channel presents two main backgrounds. The first background source is composed of the non-resonant  $ZZ \rightarrow 4l$  process, where  $ZZ$  or  $Z\gamma^*$  produce the four-lepton final state via  $q\bar{q}$  annihilation and gluon fusion. This background is called irreducible because it produces the same final state as the signal. The reducible background, which produces a different final state which can be mis-identified as a  $H \rightarrow 4l$  final state, is composed of  $Z + \text{jets}$ ,  $t\bar{t}$  and  $WZ + \text{jets}$  processes. This background contains non-isolated leptons coming from heavy-flavor quark decays ( $b$  quarks in the  $t\bar{t}$  decay), mis-reconstructed jets (in  $Z + \text{jets}$  and  $WZ + \text{jets}$  processes) and electrons from photon conversions. Since the gluon-gluon fusion production mechanism is dominant in the whole mass range, it is the process considered in this study; moreover, to understand the performances of the muon detector, the four muon final state has been studied.

#### 4. – Detector simulation

To evaluate the performances of the detector with or without the upgrades, different simulations of the CMS detector have been implemented:

- *Phase-I detector* (BX = 25 ns, PU 50,  $L = 2 \cdot 10^{34} \text{ cm}^{-2}\text{s}^{-1}$ ): condition of the detector after the Phase-I Upgrade, without radiation aging, to establish a reference for the Phase-II detector performances;
- *Phase-I detector “aged”* (BX = 25 ns, PU 140,  $L = 5 \cdot 10^{34} \text{ cm}^{-2}\text{s}^{-1}$ ): condition of the detector after  $\sim 3$  years of HL-LHC with the modeling of the radiation damage to the detector after an integrated luminosity of  $1000 \text{ fb}^{-1}$ , in order to understand if physics studies are possible without any improvement of the detector;
- *Phase-II detector* (BX = 25 ns, PU 140,  $L = 5 \cdot 10^{34} \text{ cm}^{-2}\text{s}^{-1}$ ): simulation of the detector response with all the upgrades and acceptance extensions.

Samples of  $gg \rightarrow H \rightarrow ZZ^{(*)} \rightarrow 4\mu$  were produced using the POWHEG NLO generator and Pythia 6 for event generation and fragmentation, respectively. The result is a collection of generated final state particles which represent the physics process. After the generation of the events, the interaction of the particles with the detector has to be simulated. This process has been done in two different ways for the three detector configurations.

The Phase-I and Phase-I “aged” samples have been simulated using the *Full Simulation* of CMS which is performed by GEANT 4 [16]. This tool is based on a rich set of physics models that allow a complete modeling of the particle interaction with the detector material, including a detailed description of the particle energy loss, the detector geometry, the magnetic field, the electronic response.

The Phase-II samples have been simulated using a modular framework for a fast and parametrized multi-purpose detector simulation called *Delphes* [17]. For

phenomenological studies, such as the comparison between several different configurations of the detector, the Full Simulation is too demanding in terms of computing time and resources, so a parametrized and faster approach is preferred. The Delphes simulation takes into account a tracking system embedded in a magnetic field, electromagnetic and hadron calorimeters with their granularity, and a muon identification system, reconstructing all the main physics objects. As it is parametrized, it has the limitation not to describe the material of the detector and the interaction of the particles with it. For this reason, it has been fully validated comparing the result of the Delphes simulation to the Full Simulation ones, and then used to simulate the Phase-II scenario, exploiting single muon and electron efficiency and transverse-momentum resolutions.

## 5. – Analysis and results

The same analysis used in 2012 for the Higgs boson discovery has been applied.

For the event selection, muons are accepted with  $p_T > 5 \text{ GeV}$  and pseudo-rapidity  $|\eta| < 2.4$  except for the Phase-II scenario on which the pseudo-rapidity is extended to  $3.0$ <sup>(1)</sup>. At least four isolated muons are required to be reconstructed and identified inside the acceptance of the detector. Among all opposite charged-muons pairs, the one with the invariant mass closest to the nominal  $Z$  boson mass is selected to reconstruct the first  $Z_1$ , on shell. Then among the remaining pairs, the highest  $p_T$  one is selected to reconstruct the second  $Z$  boson,  $Z_2$ . After kinematic cuts, the Higgs boson is reconstructed with the four-muons selected previously for  $Z_1$  and  $Z_2$ . The same analysis described above has been applied to the irreducible background *i.e.*  $ZZ \rightarrow 4\mu$ ; instead, the reducible background *i.e.*  $Z + jets$  has been treated with a data-driven approach. Both background studies are still ongoing.

In fig. 4 the percentage of events passing each step of the selection is shown. The signal efficiencies for the three detector configurations have been compared, restricting the pseudo-rapidity acceptance to 2.4 for the Phase-II configuration to have a correct equivalence in the geometry. The “aged” scenario shows a final event selection efficiency of  $\sim 10\%$ , clearly lower than the reference scenario ( $\sim 30\%$ ). The Phase-II configuration instead leads to a final efficiency of  $\sim 35\%$ , greater than the reference scenario without even exploiting the coverage extension. In fig. 5 the four-muons signal and irreducible background invariant mass distributions, computed at the end of the event selection, are reported for the “aged” and Phase-II configurations. From this plot too, as expected, the “aged” scenario shows the worst performances, with a degraded events selection efficiency. Instead, the improvement on the single muon reconstruction efficiency and resolution obtained with the Phase-II upgraded detector results into a better four muon invariant mass reconstruction and a larger yield of signal events.

In order to understand the effect of an extended geometry on the event selection, the Phase-II signal samples have been processed for different pseudo-rapidity values:  $|\eta| < 2.4, 3.0, 3.5$  and  $4.0$ . In fig. 6 the selection efficiency at each step of the analysis has been reported for the four configurations: a significant increase in the signal efficiency extending the muon detector coverage to large pseudo-rapidity values is clearly visible. From the lower to the greater  $\eta$  configuration, the final efficiencies

---

<sup>(1)</sup> Although the current limit on the muon system extension is 2.8, when the analysis has been performed it was at 3.0: this is the reason why in all the plots and legends  $|\eta| < 3.0$  is required.

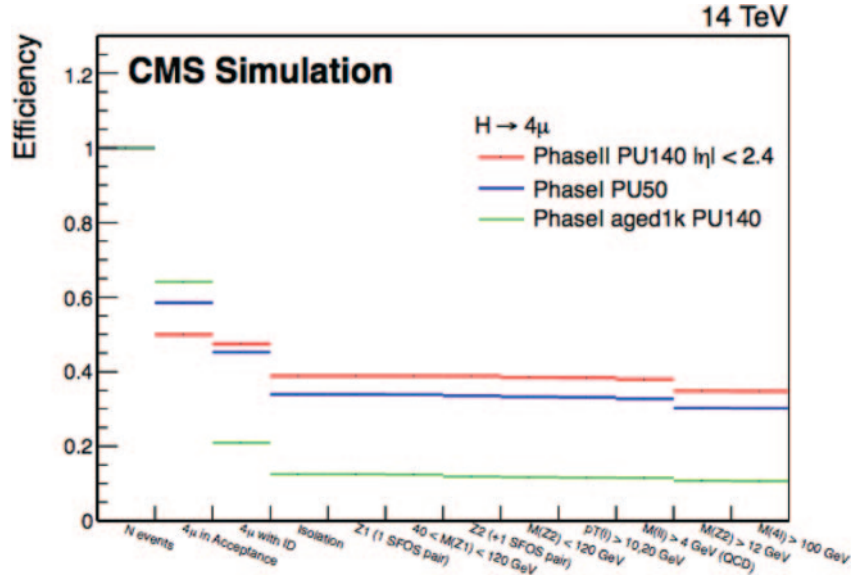


Fig. 4. – Cut flow table showing the event selection efficiency at each step of the analysis for signal  $H \rightarrow ZZ^{(*)} \rightarrow 4\mu$  for Phase-II, reference Phase-I and “aged” configurations.

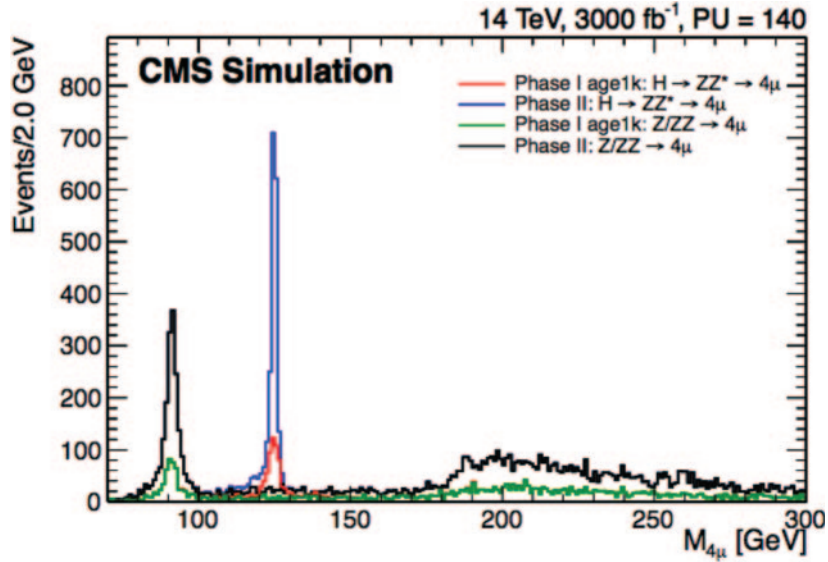


Fig. 5. – Four muons invariant mass distributions for the signal  $H \rightarrow ZZ^{(*)} \rightarrow 4\mu$  and the background  $ZZ \rightarrow 4\mu$  both for the “aged” and Phase-II configurations.

are:  $\sim 37\%$ ,  $\sim 44\%$ ,  $\sim 47\%$ ,  $\sim 49\%$ . In fig. 7 the four-muons signal and irreducible background invariant mass distributions are shown for the  $|\eta| < 2.4$  and  $|\eta| < 3.0$ : the Phase-II detector with the extended geometrical coverage shows a 20% larger acceptance with respect to the one obtained with  $|\eta| < 2.4$ .

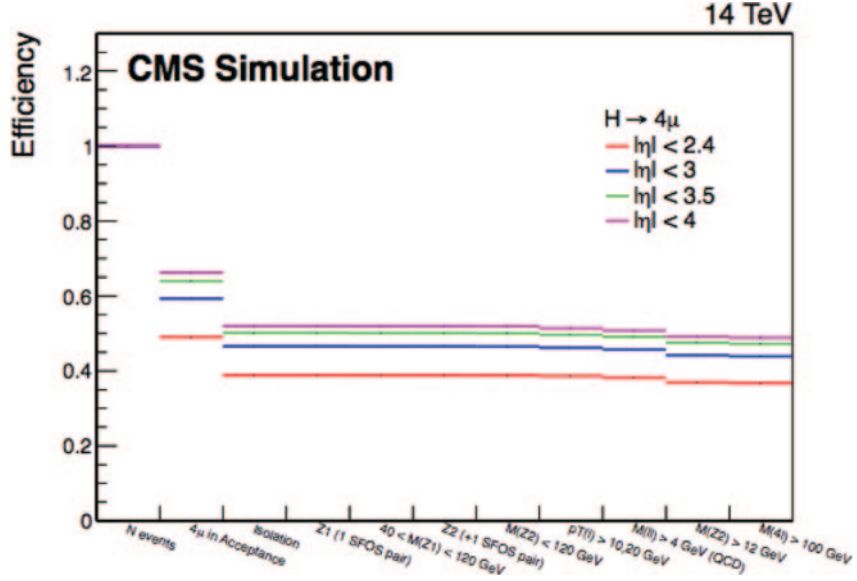


Fig. 6. – Cut flow table showing the event selection efficiency at each step of the analysis for signal  $H \rightarrow ZZ^{(*)} \rightarrow 4\mu$  for Phase-II configuration in different coverage scenarios:  $|\eta| < 2.4$ , 3.0, 3.5, 4.0.

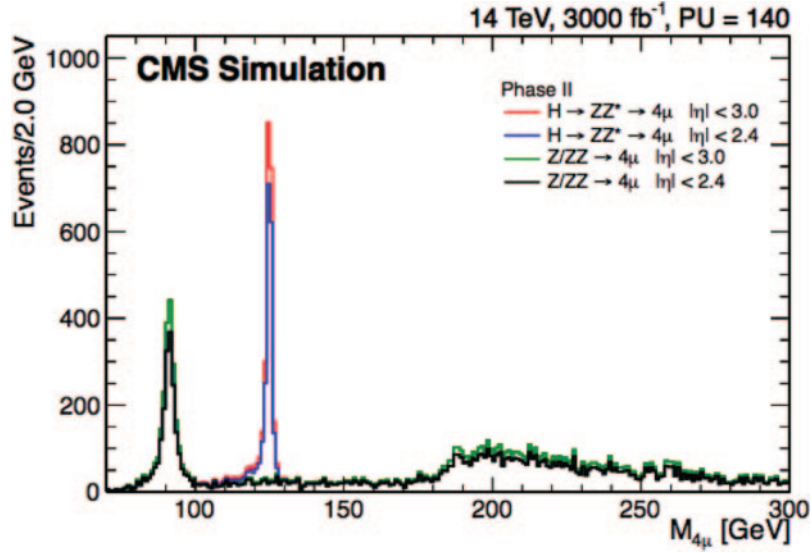


Fig. 7. – Four muons invariant mass distributions for the signal  $H \rightarrow ZZ^{(*)} \rightarrow 4\mu$  and the background  $ZZ \rightarrow 4\mu$  both for the coverage limited to  $|\eta| < 2.4$  and  $|\eta| < 3.0$ .

## 6. – Conclusions

To cope with the challenging conditions that will be imposed by the High-Luminosity LHC, the CMS experiment will undergo a substantial upgrade, referred to as Phase-II. The impact of the Phase-II CMS detector upgrade on the  $H \rightarrow ZZ^{(*)} \rightarrow 4\mu$  analysis

has been studied, comparing the results of the Higgs analysis in three different scenarios. These configurations have been simulated with Monte Carlo tools to define the CMS muon detector upgrade, that will be realized with new detectors and technologies under study, Micro-Pattern Gaseous detectors, such as GEM and  $\mu$ -RWell. The Phase-II detector performances were compared to that of the Phase-I detector (used as reference) and to another future scenario corresponding to the Phase-I detector affected by the aging and without any upgrade. The Phase-I reference detector configuration and the Phase-I “aged” configuration were simulated with the CMS Full Simulation. The parametrized Delphes framework was instead used to simulate the Phase-II detector, presenting new muon detectors to increase redundancy and extend the geometrical coverage of the muon system in the high pseudo-rapidity region. From the results obtained, two main conclusions are derived. The performances of the “aged” detector are significantly worse than the other two configurations: in order to maintain a high efficiency in the selection of Higgs events, an upgrade of the detector is mandatory. This goal can be achieved with the Phase-II detector upgrade, capable of coping with the HL-LHC challenging conditions. The event selection efficiency would increase, leading to a better Higgs invariant mass reconstruction. Furthermore, the extension in acceptance increases the final selection efficiency by 20% with respect to the Phase-II upgrade without the extended coverage.

## REFERENCES

- [1] THE ATLAS COLLABORATION, *Phys. Lett. B*, **716** (2012) 1.
- [2] THE CMS COLLABORATION, *Phys. Lett. B*, **716** (2012) 30.
- [3] ENGLERT F. and BROUT R., *Phys. Rev. Lett.*, **13** (1964) 321.
- [4] HIGGS P. W., *Phys. Lett.*, **12** (1964) 132.
- [5] THE CMS COLLABORATION, *CMS Technical Design Report for the Level-1 Trigger Upgrade*, CMS-TDR-12 (2012).
- [6] THE CMS COLLABORATION, *CMS Technical Design Report for the Phase 1 Upgrade of the Hadron Calorimeter*, CMS-TDR-010 (2012).
- [7] THE CMS COLLABORATION, *CMS Technical Design Report for the Pixel Detector Upgrade*, CMS-TDR-11 (2012).
- [8] THE CMS COLLABORATION, *Technical Proposal for the Phase-II Upgrade of the CMS Detector*, CMS-TDR-15-02 (2015).
- [9] THE CMS COLLABORATION, *CMS Phase II Upgrade Scope Document*, CERN-LHCC-2015-19 (2015).
- [10] THE CMS COLLABORATION, *The CMS Physics Technical Design Report, Volume I: Detector Performance and Software*, CERN/LHCC 2006/001 CMS Technical Design Report 8.1 (CERN) 2006.
- [11] THE CMS COLLABORATION, *The CMS Physics Technical Design Report, Volume II: Physics Performance*, CERN/LHCC 2006/021 CMS Technical Design Report 8.2 (CERN) 2006.
- [12] SAULI F. and SHARMA A., *Annu. Rev. Nucl. Part. Sci.*, **49** (1999) 341.
- [13] SAULI F., *Nucl. Instrum. Methods A*, **386** (1997) 531.
- [14] SAULI F., *Nucl. Instrum. Methods A*, **805** (2016) 2.
- [15] BENCIVENNI G., DE OLIVEIRA R., MORELLO G. and POLI LENER M., *JINST*, **10** (2015) P02008.
- [16] GEANT4 COLLABORATION (AGOSTINELLI S. *et al.*), *Nucl. Instrum. Methods A*, **506** (2003) 250.
- [17] DELPHES 3 COLLABORATION (DE FAVEREAU J. *et al.*), *JHEP*, **02** (2014) 057.